



SCUOLA INTERNAZIONALE SUPERIORE DI STUDI AVANZATI

SISSA Digital Library

Anisotropy of the superconducting fluctuations in multiband superconductors: The case of LiFeAs

Original

Anisotropy of the superconducting fluctuations in multiband superconductors: The case of LiFeAs / Fanfarillo, L., Benfatto, L.. - In: SUPERCONDUCTOR SCIENCE & TECHNOLOGY. - ISSN 0953-2048. - 27:12(2014), pp. 1-7. [10.1088/0953-2048/27/12/124009]

Availability:

This version is available at: 20.500.11767/98553 since: 2019-07-18T19:46:50Z

Publisher:

Published

DOI:10.1088/0953-2048/27/12/124009

Terms of use:

Testo definito dall'ateneo relativo alle clausole di concessione d'uso

Publisher copyright

IOP- Institute of Physics

This version is available for education and non-commercial purposes.

note finali coverpage

(Article begins on next page)

Anisotropy of the superconducting fluctuations in multiband superconductors: the case of LiFeAs

L. Fanfarillo¹ and L. Benfatto²

¹*Instituto de Ciencia de Materiales de Madrid, ICMM-CSIC,
Cantoblanco, E-28049 Madrid, Spain*

²*CNR-ISC and Dipartimento di Fisica, "Sapienza" University of Rome,
Piazzale A. Moro 2, 00185, Rome, Italy*

(Dated: October 2, 2018)

Between the different families of pnictide multiband superconductors, LiFeAs is probably one of the less understood. Indeed, despite the large amount of experiments performed in the last few years on this material, no consensus has been reached yet on the possible pairing mechanism at play in this system. Here we focus on the precursor effects of superconductivity visible in the transport experiments performed above T_c . By analyzing the superconducting fluctuations in a layered multiband model appropriate for this material, we argue that the strong two-dimensional character of the paraconductivity above T_c points towards a significant modulation of the pairing interactions along the z direction. We also discuss the peculiar differences between single-band and multi-band superconductors for what concerns the anisotropy of the superconducting-fluctuations effects above and below T_c .

I. INTRODUCTION

After the original discovery of superconductivity in LaOFeAs¹ the investigation of iron-based superconductors has led to the discovery of several classes of compounds that all display a high-temperature superconductivity, despite the fact that the different lattice structures can lead to significant differences in the electronic properties^{2,3}. Such differences justify the on-going debate on the existence of an universal pairing mechanism in all iron-based superconductors. One of the crucial questions concerns the role of antiferromagnetic spin fluctuations. Indeed, while they represent a plausible candidate for the pairing glue in those systems, as 122 compounds, with good nesting conditions between the hole and electron Fermi pockets³⁻⁵, their relevance in other systems with poor nesting properties is often questioned⁶⁻⁹. A typical example of such a system is LiFeAs. This compound is a stoichiometric superconductor with a $T_c \sim 17$ K¹⁰ and no magnetic ordering. Due to its stoichiometric nature and its clean, charge neutral cleaved surface LiFeAs is the best candidate to perform both bulk- and surface-sensitive measurements. However, the large amount of experimental findings accumulated so far did not succeed yet to clarify the nature of the pairing mechanism, but offered instead a puzzling and somehow contradictory scenario. The Fermi surface (FS) of LiFeAs observed by angle-resolved photoemission spectroscopy (ARPES) consists of two hole pockets at Γ and two electron pockets at M ¹¹⁻¹³, as in all pnictides families. However, there are some remarkable quantitative differences, which are only partly accounted for by LDA+DMFT (Dynamical Mean Field Theory) calculations^{14,15}. In particular, the FS nesting is relatively poor and the hole pockets are much shallower than in other families, with associated larger density of states (DOS) which has been suggested to pro-

mote ferromagnetic fluctuations instead of the antiferromagnetic ones⁸. Nonetheless, as stressed by several authors, despite the poor nesting, a spin-fluctuation mediated pairing^{14,18-20}, or more generically a strong interband nature of the interaction²¹, cannot be excluded. Indeed, while perfect nesting is required to have a long-ranged SDW instability (absent in LiFeAs), the presence of large spin fluctuations is sufficient to justify a spin-mediated pairing mechanism, leading to a s^\pm order parameter. Such large magnetic fluctuations in LiFeAs have been observed by nuclear magnetic resonance²² and neutron scattering experiments^{16,17}, that also identified a magnetic vector slightly incommensurate¹⁷ with respect to the $\mathbf{Q} = (\pi, \pi)$ wavevector, due probably to the bad nesting condition of the FS. While these findings can support a s^\pm scenario, its agreement with the ARPES data on the gap modulation is still under scrutiny^{12,23,24}. Also the quasiparticle interference patterns observed in scanning tunneling microscopy²⁵⁻²⁷ are subject of an intense debate. In this case different assumptions on the impurity scattering mechanism can make the experimental results compatible either with a s^\pm or with a (triplet) p -wave^{26,27} symmetry of the order parameter.

The anomalies of LiFeAs are not restricted to the superconducting (SC) state but extend up to the so called normal state. The phenomenology and in particular the dimensionality of SC fluctuations above T_c is an highly debated issue for all pnictides²⁸. However the situation in LiFeAs is particularly puzzling. Indeed, while electronic properties of LiFeAs are believed to have an almost three-dimensional (3D) character¹⁵, as confirmed by de Haas van Alphen experiments^{29,30}, the superconducting fluctuations (SCF) exhibit a marked two-dimensional (2D) fluctuation regime, which extends up to temperatures very near to T_c ^{31,32}. At the same time, the measurements of the upper critical field³³ slight below T_c would point instead to a small anisotropy between in-plane and out-of-plane SCF, at odd with paraconductivity results.

As we discuss in the present manuscript, the apparent contradictions between these results can be reconciled by taking into account both the multiband structure of pnictides and the peculiar interband character of the interactions. In particular, in multiband systems the link between the band structure and the nature of SCF, both above and below T_c , can be more involved than what expected in the single-band case, as pointed out in different contexts in the recent literature.³⁴⁻³⁷ At the same time the interband character of the pairing can lead to remarkable qualitative differences with respect to single-band systems, as it has been emphasized in the context of transport³⁸ and optical properties above T_c ³⁹. In the present work we analyze the SCF above T_c in LiFeAs by taking the point of view of a spin-mediated interband pairing mechanism, whose properties can be deduced by the analysis of the SCF themselves. We show that the microscopic estimate of the crossover temperature from 2D to 3D regime for the SCF is controlled by three cooperative mechanisms: (i) the interband nature of the pairing, which leads to a weighted contribution of the various bands in the single collective mode which controls the critical SCF³⁴; (ii) the low-energy renormalization effects beyond Density Functional Theory (DFT), due the exchange of spin fluctuations³⁹; (iii) the anisotropy of the pairing, that can make the SCF quasi-2D even for quasi-3D band dispersions. On this respect our work supports recent theoretical attempts^{19,21} to reproduce the measured gap hierarchy by taking into account the possible variations of the pairing interaction along z , due to the evolution of the FS. Our main finding is that the marked 2D character of SCF points towards a prevalent 2D nature of the spin-fluctuation mediated pairing interaction, that seems consistent with experimental observation of the magnetic fluctuations above T_c ^{22,31}. Such a result is not inconsistent with other estimates of the SC-properties anisotropy done below T_c with different probes, as the upper critical field³³, the thermal conductivity⁴⁰ and the critical current⁴¹. Indeed, as we discuss below, in a multiband superconductor the weight of the various bands to the SCF depends on the quantity under scrutiny, leading to different results in the various experimental set-up. Finally, while our findings cannot exclude an alternative pairing scenario based either on ferromagnetic⁸ or orbital⁹ fluctuations, the predominant *intra*band character of these mechanisms seems more difficult to reconcile with an anisotropic pairing mechanism, crucial to interpret the SCF above T_c .

II. COLLECTIVE CRITICAL MODE

Let us first of all summarize the expected result for the SCF anisotropy on the basis of the derivation of Ref. [34], that was done under the following hypotheses: (i) the interaction has a predominant interband character and (ii) the pairing is isotropic in momentum space (so it has the same strength at all k_z values). In this situation, it has

been demonstrated that despite the presence of multiple FS the effective action of the SCF is still characterized by the emergence of a single critical collective mode that in the case of a layered superconductor is described by the propagator:

$$L^{-1}(\mathbf{q}, \omega_m) = \nu \left[\epsilon + \eta_{\parallel} q_{\parallel}^2 + r_z \sin(q_z d/2) + \gamma |\omega_m| \right] \quad (1)$$

where ν is the effective DOS of the collective mode at the Fermi level, η_{\parallel} and r_z are the in-plane and the out-of-plane stiffness respectively, $\epsilon = \ln(T/T_c)$ and we used a periodic notation for the q_z dispersion, with d interlayer spacing. As a consequence the resulting expression for the paraconductivity is the same obtained for a single-band layered superconductor⁴², i.e.

$$\delta\sigma = \frac{e^2}{16\hbar d \sqrt{\epsilon(\epsilon + r_z)}}. \quad (2)$$

The crossover from 2D behavior $\delta\sigma \sim 1/\epsilon$ to 3D one $\delta\sigma \sim 1/\sqrt{\epsilon}$ occurs at the temperature where $\epsilon \lesssim r_z$. In LiFeAs the 2D behavior is preserved until $\epsilon \sim 0.02$, so that one deduces that the out-of-plane stiffness r_z is very small. In the single-band case the in-plane η and out-of-plane r_z stiffness can be estimated microscopically from the values of the in-plane velocity and out-of-plane hopping⁴²:

$$\eta \sim \frac{v_F^2}{T^2}, \quad r_z \sim \frac{t_z^2}{T^2}. \quad (3)$$

In the multiband case the contribution of each band to the critical-mode values for η_{\parallel} and r_z depends in general on the relative strength of intra- vs inter-band pairing^{34,43}. However, in the case of pnictides the assumption of a predominant interband coupling simplifies considerably the description of the critical collective mode. Following Ref. [34] we shall consider a four-band model with only interband pairing. By taking into account DFT calculations¹⁵ and ARPES evidences^{11,12} for LiFeAs we will consider two electronic γ_1, γ_2 bands degenerate, and two hole bands α and β , corresponding to the inner and outer hole pockets, respectively. The larger coupling λ occurs between the quasi-nested α and γ_i bands, while the $\beta - \gamma$ coupling $\lambda_{\beta\gamma} = \kappa\lambda$, $\kappa < 1$ is assumed to be smaller due to the larger size of the β pocket. The BCS-like Hamiltonian of the model is

$$H = \sum_i H_0^i + \lambda \sum_{\mathbf{q}} \left[\Phi_{\gamma, \mathbf{q}}^\dagger (\Phi_{\alpha, \mathbf{q}} + \kappa \Phi_{\beta, \mathbf{q}}) + h.c. \right]. \quad (4)$$

Here $H_0^i = \sum_{\mathbf{k}} \xi_{\mathbf{k}}^i c_{i, \mathbf{k}\sigma}^\dagger c_{i, \mathbf{k}\sigma}$, $c_{i, \mathbf{k}\sigma}^{(\dagger)}$ annihilates (creates) a fermion in the $i = \alpha, \beta, \gamma_1, \gamma_2$ band and $\xi_{\mathbf{k}}^i$ is the layered 3D band dispersion with respect to the chemical potential

$$\xi_{\mathbf{k}}^i = \frac{\mathbf{k}_{\parallel}^2}{2m_i} - t_{i,z} \cos(k_z d) - \mu. \quad (5)$$

In Eq. (4) $\Phi_{i, \mathbf{q}} = \sum_{\mathbf{k}} c_{i, \mathbf{k}+\mathbf{q}} c_{i, \mathbf{k}}$ is the pairing operator in the i -th band, with $\Phi_{\gamma, \mathbf{q}} \equiv \Phi_{\gamma_1, \mathbf{q}} + \Phi_{\gamma_2, \mathbf{q}}$. It is possible to recast the four-band model defined in Eq. (4) in an

effective two-band model by introducing the pairing operators $\Phi_e \equiv \Phi_\gamma$ and $\Phi_h \equiv \Phi_\alpha + \kappa\Phi_\beta$ so that the pairing term reads:

$$H_I = \lambda \sum_{\mathbf{q}} (\Phi_1^\dagger \Phi_2 + h.c.). \quad (6)$$

Once established the pairing model according to Eq. (6), we will use band parameters consistent with LDA+DMFT and experimental measurements,^{11,12,14,15} and we will choose the interaction strength in order to reproduce the experimental gap values. The estimate of the fluctuation regime will then follow by the explicit calculation of the critical multiband mode, done according to the analysis of Ref. [34]. Notice that despite the repulsive nature of the interaction (6) a superconducting instability is still possible in the s_\pm symmetry, where the gap changes sign between hole and electron bands. However, in contrast to the ordinary intraband-dominated pairing (as, e.g., in MgB_2 ⁴³) here a single pairing channel exists, with important consequences on the implementation of the standard procedure to derive the effective action for the SC fluctuations both above³⁴ and below³⁷ T_c . In particular, one can show that in the model (4)-(6) the contribution of the various bands to the single critical mode (1) is given by:

$$\eta_{\parallel} = (w_h^2 \eta_h + w_e^2 \eta_e), \quad r_z = (w_h^2 r_h + w_e^2 r_e) \quad (7)$$

where the coefficients w_e, w_h are fixed by the two conditions:

$$w_e w_h = 1, \quad (8)$$

$$\frac{w_e^2}{w_h^2} = \frac{\Delta_e^2}{\Delta_h^2} = \frac{\Pi_h(q=0)}{\Pi_e(q=0)}, \quad (9)$$

where $\Pi_h \equiv \Pi_\alpha + \kappa^2 \Pi_\beta, \Pi_e = 2\Pi_\gamma$ are the Cooper particle-particle bubbles evaluated at zero frequency and momentum ($q = (i\omega_n, \mathbf{q})$), $\Delta_h \equiv \Delta_\alpha = \Delta_\beta/\kappa$ and $\Delta_e \equiv \Delta_\gamma$. The last relation of Eq. (9) has been derived from the usual saddle-point equations $\Delta_e = -\lambda \Pi_h \Delta_h$ and $\Delta_h = -\lambda \Pi_e \Delta_e$. Analogously, the SCF parameters $\eta_{e(h)}, r_{e(h)}$, which are obtained by the small \mathbf{q} expansion of the Cooper bubbles (see below), are given in term of the band stiffnesses as

$$\eta_e = 2\eta_\gamma, \quad \eta_h = \eta_\alpha + \kappa^2 \eta_\beta, \quad (10)$$

$$r_e = 2r_\gamma, \quad r_h = r_\alpha + \kappa^2 r_\beta, \quad (11)$$

In first approximation the coefficients η_i and r_i can be extracted from the band parameters, listed in Table I, according to Eq. (3). For what concerns the relative weights $w_{e,h}$ in Eq. (7) one can extend the relation (9) above T_c where $\Pi_i \simeq \nu_i \ln(\omega_0/T_c)$, i.e. each band is weighted inversely proportional to its DOS ν_i . By means of Eqs. (7), (9) and (11), and by using the band parameters listed in Table I, extracted from LDA+DMFT and experimental measurements,^{11,12,14,15} we can provide a preliminary estimate of the anisotropy parameter r_z for LiFeAs. As one

can see in Table I, even though the outer hole band has $t_z \approx 0$, the t_z in the inner hole band and in the electron ones is quite larger, of order of 15 meV. As a consequence from Eq.(3) one expects a value $r_z \sim \mathcal{O}(10)$ even considering the weighting factors w_e, w_h defined in Eq. (7) to compute the average r_z of the critical collective mode. Such an estimate can be hardly reconciled with the experimental observation of a 2D regime for the SCF up to very small $\varepsilon \sim 0.02$, that would imply $r_z \sim 10^{-2}$.

	α	β	γ_1, γ_2
m/m_e	4.51	5.86	3.68
t (meV)	58	45	72
ν (eV) ⁻¹	1.37	1.77	1.11
ε^0 (meV)	33	112	-68
t_z (meV)	15	0	17
Δ (meV)	6.0	3.4	3.6

TABLE I: LiFeAs is a layered system (lattice parameters $a \sim 3.9$ Å, $d \sim 6.5$ Å). The relevant bands near the Fermi level α, β, γ can all be approximated according to Eq.(5). m is the in-plane mass, t the in-plane hopping, ν the density of state, t_z the out-of-plane hopping, $\varepsilon^0 = \varepsilon_{min}^e, \varepsilon_{max}^h$ the band edge and Δ the gap. The band parameters and the gap values are extracted from [11,12,14,15]. The weighting factors $w_{e,h}$ in Eq. (7) are determined by the band DOS, according to the relation (9). The gap values can be used instead to tune the superconducting couplings λ and $\lambda\kappa$, see Eq. (6).

III. ANISOTROPY OF THE PAIRING INTERACTION

All the above discussion has been based on the idea that the anisotropy of SCF is simply determined by the anisotropy of the band structure, and band parameters have been extracted from LDA+DMFT and ARPES measurements. In this Section we discuss how this estimate can be modified by taking into account several properties peculiar to pnictides. A first correction to be considered is the low-energy band renormalization due to the same spin fluctuations that mediate the pairing. Indeed, while LDA+DMFT correctly accounts for the high-energy effects (like Hubbard- U interactions) that renormalize the overall bandwidth, spin fluctuations can give rise to an additional band renormalization visible in a small energy range (of the order of the spin-fluctuation scale $\omega_0 \sim 10 - 20$ meV) around the Fermi level. The dichotomy between these two effects has been discussed for example in Ref. [39], where it has been show how these low-energy renormalization effects are crucial to understand the discrepancy between the effective masses probed by ARPES and the thermodynamical probes, sensible to the carrier mass at the Fermi level. By using the results of an Eliashberg-like approach to the spin-mediated interactions one can then introduce an addi-

tional reduction of the hopping parameters listed in Table I as $t_i \rightarrow t_i/(1 + \lambda)$, where λ represents here an average dimensionless coupling to spin fluctuations, estimated³⁹ to be in the intermediate-coupling regime $\lambda \sim 1 - 2$. By including this effect we already reduce r_z to $\simeq 2$, that is however still much larger than the experimental value. A second aspect to be considered is the modulation of the pairing interaction along k_z . Indeed, it is well known that in the case of pnictides the structure of the pairing interaction along k_z can be definitively much more involved, as it has been recently pointed out in the case of P-doped BaFeAs⁴⁵. By assuming that the pairing originates mainly from a spin-fluctuations mediated interband mechanism, one must consider the evolution along the z direction both of the orbital character of the bands and of the nesting properties between the (anisotropic) hole and electron pockets, that contribute both to the effective k_z dependence of the pairing interaction. Both properties can vary between different materials and also as a function of doping. For example, in Co-doped BaFeAs it has been experimentally shown that spin fluctuations that are 3D anisotropic in the undoped compound become much more 2D in the optimally-doped one, where a 2D picture seems then more appropriate⁴⁶. Even though a detailed experimental investigation of this issue on LiFeAs is not yet available, there have been already suggestions^{19,21} for a possible k_z dependence of the pairing interactions induced by the variations of the FS topology along z . We analyze here the consequences on a anisotropic pairing interaction along k_z for the properties of the SCF. In this case, while the structure (1) of the critical collective mode does not change, we must reconsider the estimate (3) of the single-band parameters when the pairing has an anisotropic structure along k_z . On very general grounds^{34,42,43} the SCF stiffnesses η_i, r_i are extracted from the small \mathbf{q} expansion of the Cooper bubbles in each band. If one introduces explicitly a modulation function $w(k_z)$, that accounts for the variation of the pairing interaction along the z -axis, the Cooper bubble is:

$$\begin{aligned} \Pi_i(\mathbf{q}, 0) &= \frac{T}{N} \sum_{\mathbf{k}, i\omega_n} w^2(k_z) G_i(\mathbf{k} + \mathbf{q}, \omega_n) G_i(-\mathbf{k}, -\omega_n) = \\ &= \frac{1}{N} \sum_{\mathbf{k}} w^2(k_z) \frac{f(-\xi_{\mathbf{k}}^i) - f(\xi_{\mathbf{k}+\mathbf{q}}^i)}{\xi_{\mathbf{k}}^i + \xi_{\mathbf{k}+\mathbf{q}}^i}, \end{aligned} \quad (12)$$

where G_i is the Green's function of the i -th band above T_c . By retaining leading terms in the \mathbf{q}^2 expansion on Eq. (12) one obtains:

$$\begin{aligned} \nu_i \eta_i &= \frac{1}{8N} \sum_{\mathbf{k}} w^2(k_z) v_{i,\parallel}^2(\mathbf{k}) \left[\frac{f'(\xi_{\mathbf{k}}^i)}{(\xi_{\mathbf{k}}^i)^2} + \frac{\tanh(\beta \xi_{\mathbf{k}}^i/2)}{2(\xi_{\mathbf{k}}^i)^3} \right], \\ \nu_i r_i &= \frac{1}{4N} \sum_{\mathbf{k}} w^2(k_z) v_{i,z}^2(\mathbf{k}) \left[\frac{f'(\xi_{\mathbf{k}}^i)}{(\xi_{\mathbf{k}}^i)^2} + \frac{\tanh(\beta \xi_{\mathbf{k}}^i/2)}{2(\xi_{\mathbf{k}}^i)^3} \right], \end{aligned} \quad (13)$$

where $\mathbf{v}_{\mathbf{k}} = \partial \xi_{\mathbf{k}} / \partial \mathbf{k}$, so that for a band dispersion as in Eq. (5) $v_{\parallel}(\mathbf{k}) = \partial_{\mathbf{k}_{\parallel}} \xi_{\mathbf{k}}$ and $v_z \sim \sin k_z$. The \mathbf{k} -integrals in Eqs. (13)-(13) are dominated by $\mathbf{k} = (\mathbf{k}_{\parallel}, k_z)$ values at the FS. In particular for $w^2(k_z) = 1$ one recovers the usual estimates (3), so that r_z scales as t_z . However, when $w^2(k_z)$ is peaked at small k_z values, where $v_z \sim 0$, and it is reduced at intermediate $k_z d \simeq \pi/2$, where v_z is maximum, the effective out-of-plane parameter r_z will be strongly suppressed with respect to t_z . This effect is in part compensated by an analogous reduction of the effective DOS ν_i that appears as a prefactor in the expansion (13), and that is now defined as:

$$\nu_i = \int_{d\xi_i} \delta(\xi_F^i - \xi_{\mathbf{k}}^i) w^2(k_z), \quad (14)$$

while the usual band DOS would be computed with $w^2(k_z) = 1$. Since the anisotropy parameter scales as $r_z \sim \int dk_z v_z w^2(k_z) / \int dk_z w^2(k_z)$ its overall reduction is smaller than the one of the pairing-averaged out-of-plane velocity. In the following we will consider as a paradigmatic example a modulation $w_{\sigma}(k_z)$ function defined as (Fig. 1.b)

$$w_{\sigma}^2(k_z) = \exp \left[-\frac{(1 - \cos(2k_z))^2}{2\sigma^2} \right], \quad (15)$$

and we will study the evolution of the effective anisotropy parameter r_z as σ changes.

Finally, to make a closer connection to experimental data we will also account for disorder effects, that can be relevant in the regime of temperature we are considering. Indeed while weak disorder does not affect the T_c , defined by the $q = 0$ limit of the Cooper bubble, it modifies the stiffness⁴². While for the $q = 0$ limit of the Cooper bubble the inclusion of vertex corrections due to disorder is crucial, for an estimate of the stiffness we can in first approximation use the bare-bubble scheme, corresponding to replacing in Eq. (12) the bare Green's function with the one having a finite quasiparticle scattering rate Γ , and integrating over the frequency the corresponding broadened spectral functions. As a consequence, the anisotropy coefficients of Eq. (13) are replaced by:

$$\begin{aligned} \nu_i \eta_i &= \frac{1}{4N} \sum_{\mathbf{k}, k_z} w^2(k_z) v_{i,\parallel}^2(\mathbf{k}) \int dz dz' A(\xi_i, z) A(\xi_i, z') R(z, z'), \\ \nu_i r_i &= \frac{1}{2N} \sum_{\mathbf{k}, k_z} w^2(k_z) v_{i,z}^2(\mathbf{k}) \int dz dz' A(\xi_i, z) A(\xi_i, z') R(z, z'), \end{aligned}$$

where ξ_i is given by Eq. (5) and

$$\begin{aligned} A(\xi, z) &= \frac{1}{\pi} \frac{\Gamma}{(z - \xi)^2 + \Gamma^2}, \\ R(z, z') &= \frac{f'(z) + f'(-z')}{(z + z')^2} + 2 \frac{f(-z') - f(z)}{(z + z')^3}. \end{aligned}$$

The results for the effective anisotropy coefficient r_z computed for LiFeAs are shown in Fig. 1.a. Here, to

better clarify the interplay between the effects of disorder and of the anisotropy of the pairing interaction, we present a map of r_z in terms of the scattering rate Γ and of the standard deviation σ of the interaction's weight (see Fig. 1.a) The effective anisotropy parameter r_z is maximum at $\Gamma \rightarrow 0$ meV and $\sigma \rightarrow 10$, which represents the clean case and isotropic pairing interaction. Increasing the amount of disorder (i.e. increasing Γ), as well as squeezing the $w_\sigma(k_z)$ function by reducing its standard deviation σ , one observes a strong reduction of r_z . While a significant reduction of r_z can be obtained with these two cooperative mechanisms, the experimental estimate of a r_z as low as 0.02 would require a marked 2D character of the pairing mechanism, along with a non-negligible residual scattering rate $\Gamma \simeq 10$ meV. While these estimates are not inconsistent with the measured resistivity³² and with the 2D character of the spin fluctuations above T_c ^{22,31}, explaining then paraconductivity experiments^{31,32}, the comparison with the experimental findings below T_c , where the SC properties appear rather isotropic, requires a detailed discussion.

IV. COMPARISON WITH OTHER EXPERIMENTS BELOW T_c

In the previous section we showed that the quasi-2D character of the SCF above T_c in LiFeAs can be understood by taking into account the anisotropy of the pairing mechanism along the interlayer direction. A crucial issue is then to compare this result with other estimates of the SC-properties anisotropy done in the literature below T_c . Here we discuss in details three experiments measuring the upper critical field³³, the critical current⁴¹ and the thermal conductivity⁴⁰. In general, while comparing paraconductivity experiments above T_c with other probes below T_c , two main differences due to the multiband nature of the system must be taken into account. First of all, for what concerns the connection between the pairing mechanism and the SC gap below T_c , one should consider that when the pairing is mediated by spin fluctuations the Fermi-surface reconstruction due to superconductivity below T_c can reduce, within a self-consistent scheme, the anisotropy of the pairing interaction. This implies for example that the gap function below T_c can be less anisotropic than what probed by the SCF above T_c . Second, for what concerns more specifically the behavior of the SCF, for a multiband superconductor the weighted contribution of the various bands to the SCF is *not* the same for the different experimental probes, in contrast to what happens in a single-band system.

Let us start with the estimate of the anisotropy $\gamma_H = H_{c2}^\perp / H_{c2}^\parallel$ between the critical fields perpendicular and parallel to the c axis, respectively³³. By converting the critical field in the correlation length by using the standard formulas $H_{c2}^\parallel = \Phi_0^2 / 2\pi(\xi_\parallel^H)^2$ and

$H_{c2}^\perp = \Phi_0^2 / 2\pi\xi_z^H \xi_\parallel^H$ one has:

$$\gamma_H^{GL} = \frac{H_{c2}^\perp}{H_{c2}^\parallel} = \left(\frac{\xi_\parallel^H}{\xi_z^H} \right) \quad (16)$$

In a standard single-band superconductor the correlation lengths ξ_\parallel^H, ξ_x^H which enter the above formula coincide with the ones obtained by the hydrodynamic expansion of the fluctuation propagator (1). Thus, one would estimate

$$\gamma_H^{GL} = \left(\frac{4\eta_\parallel}{r_z d^2} \right)^{1/2} \quad (17)$$

Notice that since γ_H^{GL} is given by the ratio between the in-plane and out-of-plane stiffness it is rather insensitive to disorder. This is shown in Fig. 1c, where we report the expected *single-band-like* estimate (17) of γ_H^{GL} for LiFeAs both in the clean and the dirty case as a function of the pairing anisotropy. We also show in the same plot the anisotropy parameter r_z for the dirty case. As one can see, when $r_z \simeq 0.02$, that would be consistent with paraconductivity experiments above T_c , γ_H^{GL} would be around 20, i.e. much larger than the value $\gamma_H \sim 2.5$ obtained experimentally near T_c . However, in a multiband superconductor one cannot in general identify the ξ_\parallel^H, ξ_z^H entering Eq. (16) with the ones entering the paraconductivity *at zero magnetic field*. The reason is the following: the paraconductivity is determined by the hydrodynamic expansion of the SC collective mode which becomes critical at T_c at zero magnetic field. Thus, as showed in Ref. [34], one first diagonalizes the multiband problem at zero frequency and momentum to identify the contribution of the various bands to the critical SC mode. Afterwards one expands it at small momenta, to obtain the propagator (1) which enters the leading Aslamazov-Larkin diagrams contributing to the paraconductivity. To solve instead the problem at finite magnetic field one must diagonalize the multiband problem by retaining gradient terms (i.e. the finite-momentum expansion) in the GL propagator for each band. This leads in general to the identification of new multiband effective correlation lengths ξ_\parallel^H, ξ_z^H , where the various bands can contribute with different weights with respect to the zero-field case. A typical example is the two-band case with only interband pairing. The in-plane correlation length entering the paraconductivity can be deduced from Eq. (7), while the upper critical field H_{c2}^\parallel has been computed in Ref.[35], and reads

$$H_{c2}^\parallel(T) = \frac{24\pi\Phi_0 T_c(T_c - T)}{7\zeta(3)\hbar^2(v_e^2 + v_h^2)/2} = \frac{\Phi_0}{2\pi(\xi_\parallel^H)^2} \quad (18)$$

where $v_{e,h}$ are the velocities of the electron/hole bands, respectively. As a consequence, since $\xi_\parallel^2 \propto \eta_\parallel$ and $\eta_{e,h} \propto v_{e,h}^2$ from Eq. (3), we obtain:

$$\xi_\parallel^2 \sim \frac{1}{2}(w_h^2 v_h^2 + w_e^2 v_e^2), \quad (\xi_\parallel^H)^2 \sim \frac{1}{2}(v_h^2 + v_e^2). \quad (19)$$

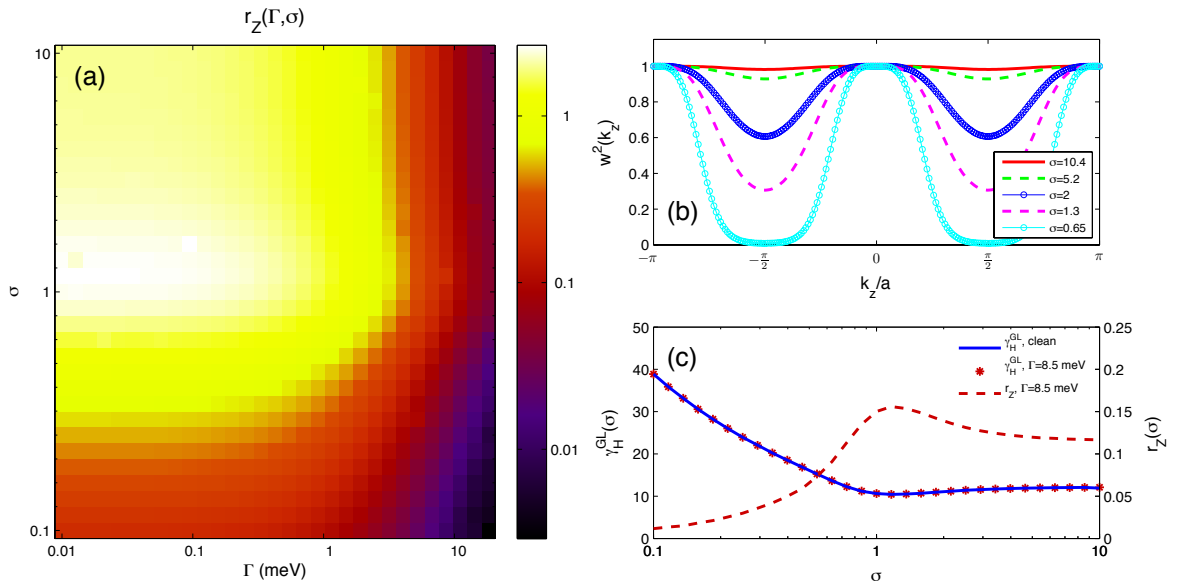


FIG. 1: (a) Dependence of the effective anisotropy parameters r_z slightly above T_c ($T \sim 18$ K) on the scattering rate Γ and on the amplitude σ of the k_z weighting function $w(k_z)$ of Eq. (15). As $\Gamma \rightarrow 0$ meV and $\sigma \rightarrow 10$ one recovers the result of the clean, isotropic limit $r_z \sim 2$. By increasing the disorder, as well as squeezing the $w_\sigma(k_z)$ function, one finds a strong and sudden reduction of r_z . (b) Parametric view of the $w_\sigma^2(k_z)$ function in the range of integration in k_z . For $\sigma = 10$ the weight $w_{\sigma=10}(k_z) \sim 1$ in the full range of integration and one recovers the standard results. (c) Single-band estimate of the Ginzburg-Landau upper critical-field anisotropy γ_H^{GL} , as given by Eq. (17), as a function of σ . The solid line and the symbols correspond to the clean and dirty case ($\Gamma = 8.5$ meV), respectively. The value of r_z for the same disorder level is also reported (dashed line).

This means in particular that the two bands contribute equally to ξ_{\parallel}^H , while this is not the case for ξ_{\parallel} . Notice also that the above estimate (18) has been done for two bands with the same mass anisotropy, which is not the case for LiFeAs. Thus, the result for a three-band model as the one used in Sec. II is not known yet, and no conclusions can be reached on the expected values of $\xi_{\parallel}^H, \xi_z^H$ in our case. We also note in passing that recently the anisotropy of the correlation length below T_c has been inferred also by measurements of the critical current at different magnetic fields⁴¹. Interestingly, these measurements show an *increase* of the γ_H ratio as the magnetic field decreases, with variations near T_c by about one order of magnitude between $H = 0.5$ T and $H \simeq H_{c2}$. This result could then could reconcile the apparent discrepancy between the paraconductivity, measured at zero field, and the upper-critical fields results.

A second interest comparison can be done with the measurements of the thermal conductivity reported in Ref.⁴⁰ Here it has been shown that the thermal transport is quite isotropic in LiFeAs, both for in-plane and out-of-plane heat current. This would rule out any possible gap node or minima for the gap both within the $k_z = 0$ plane and along the k_z direction. However, once more care should be used to interpret data in a multiband superconductor in terms of a single-band scheme. In particular heat transport in a multiband superconduc-

tor is dominated by the band with the smallest gap⁴⁴. Thus, in LiFeAs one would expect a dominant contribution coming from the β hole pocket, which is the less interacting one and then less affected by the modulation of the pairing mechanism proposed above.

V. CONCLUSIONS

In summary, we studied a microscopic layered three-band model for the SCF in LiFeAs. By using realistic band parameters, as extracted from the experiments, we showed that the strong 2D character of the SCF found experimentally can be understood as a signature of a strong anisotropy along the inter-plane direction of the pairing interaction, which compensates the low anisotropy of the band dispersion. While within a single-band scenario it would be difficult to reconcile this result with other measurements on the SC anisotropy below T_c , the multiband character of pnictides makes such a comparison not straightforward, leaving several questions open for future investigation.

VI. ACKNOWLEDGEMENTS

This work has been supported by the Italian MIUR under the project FIRB-HybridNanoDev-RBFR1236VV

and the project PRIN-RIDEIRON-2012X3YFZ2, and by the Spanish Ministerio de Economía y Competitividad (MINECO) under the project FIS2011-29680.

- ¹ Y. Kamihara, T. Watanabe, M. Hirano, and H. Hosono, *J. Am. Chem. Soc.* **130**, 3296 (2008).
- ² J.Paglione, R.L. Greene *Nature* **6**, 645 (2010)
- ³ G. R. Stewart *Rev. Mod. Phys.* **83**, 1589 (2011)
- ⁴ A. Chubukov, *Annual Review of Condensed Matter Physics* Vol. 3: 57-92 (2012)
- ⁵ P.J. Hirschfeld, M.M Korshunov, and I. Mazin *Rep. Prog. Phys.* **74**, 124508 (2011)
- ⁶ Y. Xia, D. Qian, L. Wray, D. Hsieh, G.F. Chen, J.L. Luo, N.L. Wang and M.Z. Hasan *Phys. Rev. Lett.* **103**, 037002 (2009)
- ⁷ H. Kontani and S. Onari, *Phys. Rev. Lett.* **104**, 157001 (2010);
- ⁸ P.M.R. Brydon, M. Daghofer, C. Timm, and J. van den Brink, *Phys. Rev. B* **83**, 060501 (2011).
- ⁹ T. Saito, S. Onari, Y. Yamakawa, H. Kontani, S.V. Borisenko, V.B. Zabolotnyy arXiv: 1402.2398 (2014)
- ¹⁰ M.J. Pitcher, D.R. Parker, P. Adamson, S.J.C. Herkelrath, A.T. Boothroyd, R.M. Ibberson, M. Brunelli and S.J. Clarke *Chem. Commun.* **2008**, 5918 (2008).
- ¹¹ S.V. Borisenko, V.B. Zabolotnyy, D.V. Evtushinsky, T.K. Kim, I.V. Morozov, A.N. Yaresko, A.A. Kordyuk, G. Behr, A. Vasiliev, R. Follath, B. Büchner *Phys. Rev. Lett.* **105**, 067002 (2010).
- ¹² K. Umezawa, Y. Lee, H. Miao, K. Nakayama, Z.-H. Liu, P. Richard, T. Sato, J.B. He, D.-M. Wang, G.F. Chen, H. Ding, T. Takahashi, and S.-C. Wang *Phys. Rev. Lett.* **108**, 037002 (2012).
- ¹³ T. Hajiri, T. Ito, R. Niwa, M. Matsunami, B. H. Min, Y. S. Kwon, and S. Kimura, *Phys. Rev. B* **85**, 094509 (2012)
- ¹⁴ Geunsik Lee, Hyo Seok Ji, Yeongkwan Kim, Changyoung Kim, Kristjan Haule, Gabriel Kotliar, Bumsung Lee, Seunghyun Khim, Kee Hoon Kim, Kwang S. Kim, Ki-Seok Kim, and Ji Hoon Shim, *Phys. Rev. Lett.* **109**, 177001 (2012)
- ¹⁵ J. Ferber, K. Foyevtsova, R. Valenti, H.O. Jeschke *Phys. Rev. B* **85**, 094505 (2012).
- ¹⁶ A.E. Taylor, M.J. Pitcher, R.A. Ewings, T.G. Perring, S.J. Clarke and A.T. Boothroyd, *Phys. Rev. B* **83**, 220514 (2011).
- ¹⁷ N. Qureshi, P. Steffens, Y. Drees, A.C. Komarek, D. Lamago, Y. Sidis, L. Harnagea, H.-J. Grafe, S. Wurmehl, B. Büchner, M. Braden, *Phys. Rev. Lett.* **108**, 117001 (2012).
- ¹⁸ C. Platt, R. Thomale, and W. Hanke, *Phys. Rev. B* **84**, 235121 (2011).
- ¹⁹ Y. Wang, A. Kreisel, V. B. Zabolotnyy, S. V. Borisenko, B. Büchner, T. A. Maier, P. J. Hirschfeld, and D. J. Scalapino, *Phys. Rev. B* **88**, 174516 (2013)
- ²⁰ G.A. Ummarino, Sara Galasso, D. Daghero, M. Tortello, R.S. Gonnelli, A. Sanna, *Physica C: Superconductivity*, **492**, 15 (2013)
- ²¹ F. Ahn, I. Eremin, J. Knolle, V. B. Zabolotnyy, S. V. Borisenko, B. Büchner, and A. V. Chubukov *Phys. Rev. B* **89**, 144513 (2014).
- ²² L.Ma, J.Zhang, G.F.Chen, and Weiqiang Yu *Phys. Rev. B* **82**, 180501 (2010).
- ²³ A.A. Kordyuk, V.B. Zabolotnyy, D.V. Evtushinsky, T.K. Kim, L.V. Morozov, M.L. Kulić, R. Follath, G. Behr, B. Büchner, and S.V. Borisenko, *Phys. Rev. B* **83**, 134513 (2011)
- ²⁴ S.V. Borisenko, V.B. Zabolotnyy, A.A. Kordyuk, D.V. Evtushinsky, T. K. Kim, I. V. Morozov, R. Follath, B. Büchner, *Symmetry* **4**, 251-264 (2012)
- ²⁵ Allan et. al. *Science* **336**, 563 (2012).
- ²⁶ T. Hänke, S. Sykora, R. Schlegel, D. Baumann, L. Harnagea, S. Wurmehl, M. Daghofer, B. Büchner, J. van den Brink, C. Hess, *Phys. Rev. Lett.* **108**, 127001 (2012).
- ²⁷ C. Hess, S. Sykora, T. Hänke, R. Schlegel, D. Baumann, V.B. Zabolotnyy, L. Harnagea, S. Wurmehl, J. van den Brink, B. Büchner *Phys. Rev. Lett.* **110**, 017006 (2013).
- ²⁸ see for example R.I. Rey, A.Ramos-Álvarez, C. Carballeira, J. Mosqueira, F. Vidal, S.Salem-Sugui Jr, A.D. Alvarenga, Rui Zhang, Huiqian Luo, *Supercond. Sci. Technol.* **27**, 075001 (2014) and references therein.
- ²⁹ C. Putzke, A. I. Coldea, I. Guillaumon, D. Vignolles, A. McCollam, D. LeBoeuf, M. D. Watson, I. I. Mazin, S. Kasahara, T. Terashima, T. Shibauchi, Y. Matsuda, and A. Carrington, *Phys. Rev. Lett.* **108**, 047002 (2012).
- ³⁰ B. Zeng, D. Watanabe, Q. R. Zhang, G. Li, T. Besara, T. Siegrist, L. Y. Xing, X. C. Wang, C. Q. Jin, P. Goswami, M. D. Johannes, and L. Balicas, *Phys. Rev. B* **88**, 144518 (2013)
- ³¹ Yoo Jang Song, Byeongwon Kang, Jong-Soo Rhee, Yong Seung Kwon, *Europhys. Lett.* **97**, 47003 (2012)
- ³² F. Rullier-Albenque, D. Colson, A. Forget, H. Alloul, *Phys. Rev. Lett.* **109**, 187005 (2012).
- ³³ B. Lee, S. Khim, JYoo Jang Song, Byeongwon Kang, Jong-Soo Rhee, Yong Seung Kwon *Europhys. Lett.* **91**, 67002 (2010); N. Kurita, K. Kitagawa, K. Matsubayashi, A. Kismarhardja, E.S. Choi, J.S. Brooks, Y. Uwatoko, S. Uji, T. Terashima *J. Phys. Soc. Jpn.* **80**, 013706 (2011); K. Cho, H. Kim, M.A. Tanatar, Y.J. Song, Y.S. Kwon, W.A. Coniglio, C.C. Agosta, A. Gurevich, R. Prozorov *Phys. Rev. B* **83**, 060502 (2011); S. Kasahara, K. Hashimoto, H. Ikeda, T. Terashima, Y. Matsuda, and T. Shibauchi, *Phys. Rev. B* **85**, 060503(R) (2012)
- ³⁴ L. Fanfarillo, L. Benfatto, S. Caprara, C. Castellani, and M. Grilli *Phys. Rev. B* **79**, 172508 (2009).
- ³⁵ A. Gurevich, *Phys. Rev. B* **82**, 184504 (2010).
- ³⁶ N. V. Orlova, A. A. Shanenko, M. V. Milosević, F. M. Peeters, A. V. Vagov, and V. M. Axt, *Phys. Rev. B* **87**, 134510 (2013).
- ³⁷ M. Marciani, L. Fanfarillo, C. Castellani, and L. Benfatto, *Phys. Rev. B* **88**, 214508 (2013)
- ³⁸ L. Fanfarillo, E. Cappelluti, C. Castellani, L. Benfatto, *Phys. Rev. Lett.* **109**, 096402 (2012).
- ³⁹ L. Benfatto and E. Cappelluti, *Phys. Rev. B* **83**, 104516 (2011). L. Benfatto, E. Cappelluti, L. Ortenzi and L. Boeri, *Phys. Rev. B* **83**, 224514 (2011).

- ⁴⁰ M.A. Tanatar, J.-Ph. Reid, S. Rene de Cotret, N. Doiron-Leyraud, F. Laliberte, E. Hassinger, J. Chang, H. Kim, K. Cho, Yoo Jang Song, Yong Seung Kwon, R. Prozorov, Louis Taillefer Phys. Rev. B **84**, 054507 (2011).
- ⁴¹ M. Konczykowski, C.J. van der Breek, M.A. Tanatar, V. Mosser, Yoo Jang Song, Yong Seung Kwon, R. Prozorov, Phys. Rev. B **84**, 180514 (2011).
- ⁴² A. Larkin and A. Varlamov, *Theory of fluctuations in superconductors*, (Clarendon Press, Oxford, 2005).
- ⁴³ A. E. Koshelev, A. A. Varlamov and V. M. Vinokur, Phys. Rev. B **72**, 064523 (2005).
- ⁴⁴ A. A. Golubov and A. E. Koshelev, Phys. Rev. B **83**, 094521 (2011)
- ⁴⁵ Y. Zhang, Z.R. Ye, Q.Q. Ge, F. Chen, Juan Jiang, M. Xu, B.P. Xie and D.L. Feng Nat. Phys. **8**, 371 (2012).
- ⁴⁶ M.D.Lumsden et al. Phys. Rev. Lett. **102**, 107005 (2009).